target lesions and TLR, was recorded. Coronary risk factors, comprising DM (fasting blood glucose > 126 mg/dl or glycated haemoglobin > 6.5%), hypertension (blood pressure > 130/85 mmHg), hypercholesterolaemia (total cholesterol > 220 mg/dl) and smoking, were also checked and evaluated for association with re-stenosis.

STATISTICAL ANALYSES

Continuous variables were expressed as mean ± SD and were compared using Student's *t*-test and analysis of variance. Categorical data were compared using the χ^2 test or Fisher's exact test. MACE-free survival distributions were calculated by Kaplan–Meier analysis and differences were assessed using the log-rank test. A *P*-value < 0.05 was considered statistically significant. All data analyses were performed using StatView® J 5.0 software (SAS Institute, Cary, NC, USA).

Results

A total of 7660 consecutive patients (5745 men) with 9392 lesions underwent PCI for coronary artery disease at Kanazawa University Hospital and affiliate hospitals between January 2006 and December 2008 and were eligible for enrolment into this study. Angiography was carried out in 5570 (72.7%) of these patients. Of the 9392 total number of lesions, 1233 were treated without stenting (959 using only balloon dilatation and 274 with thrombectomy or directional coronary atherectomy) so were excluded from the analysis. The remaining 8159 lesions in 6739 patients (mean ± SD age 68.9 ± 10.5 years; 5103 men) were evaluated and stenting was successful in 8129 (99.6%) lesions from 6709 (99.6%) patients. Because this was a multicentre study, with data obtained from many hospitals (see Appendix), it was not possible to obtain data on all variables for all patients.

TABLE 1:
Baseline clinical and angiographic characteristics in patients treated with a bare metal stent (BMS) or drug-eluting stent (DES) for coronary artery disease

Characteristic	BMS	DES	Statistical significance
No. of patients	2934	3805	NS
No. of lesions treated by PCI	3536	4623	NS
Acute coronary syndrome, No. (%) of total lesions	1702 (48.1)	719 (15.6)	$P < 0.0001$
Age, years, mean ± SD	68.8 ± 11.2	69.0 ± 10.0	NS
Male, *n* (%)	2230 (76.0)	2873 (75.5)	NS
Coronary risk factors, *n* (%)			
Diabetes mellitus	1171 (39.9)	1899 (49.9)	$P < 0.0001$
Hypertension	1810 (61.7)	2473 (65.0)	NS
Hypercholesterolaemia	1338 (45.6)	1750 (46.0)	NS
Current smoker	1229 (41.9)	1564 (41.1)	NS
Lesion characteristics, *n* (%)			
Single vessel	1623 (55.3)	1925 (50.6)	NS
Two vessels	760 (25.9)	1176 (30.9)	NS
Three vessels	428 (14.6)	590 (15.5)	NS
LMCA	123 (4.2)	114 (3.0)	NS

Percentages calculated on the number of patients unless stated otherwise.
PCI, percutaneous coronary intervention; LMCA, left main coronary artery; NS, not statistically significant, $P > 0.05$.

BASELINE CHARACTERISTICS

Baseline clinical and angiographic characteristics of the patients are shown in Table 1 and were similar in the BMS and DES groups with the exceptions of the number of lesions in patients with acute coronary syndrome (ACS) and the numbers of patients with DM as a coronary risk factor. A total of 2421 lesions were associated with ACS: 1702 (48.1%) and 719 (15.6%) BMS- and DES-treated lesions, respectively ($P < 0.0001$). DM was associated with 3070 patients: 1171 (39.9%) BMS-treated patients and 1899 (49.9%) DES-treated patients ($P < 0.0001$).

IN-HOSPITAL OUTCOMES

Angiographic success was obtained in 6618 (98.2%) and clinical success in 6476 (96.1%) patients. Within 30 days after the procedure, stent-related MACE were observed in 74 (1.1%) patients, including 49 (0.7%) deaths and 25 (0.4%) cases of ACS, comprising 21 (0.3%) cases of myocardial infarction and four (0.05%) cases of unstable angina associated with angiographically confirmed subacute stent thrombosis (Table 2). The frequency of MACE up to 30 days after the procedure was significantly higher in the BMS group than in the DES group ($P < 0.0001$).

LONG-TERM OUTCOMES

Re-stenosis and TLR

All cases of successful stenting (8129 lesions from 6709 patients) were clinically followed up for a period of 3 years and 5975 lesions (73.5%) underwent follow-up coronary angiography after the initial procedure (mean ± SD follow-up interval 7.3 ± 4.9 months). The number of lesions for which re-stenosis was carried out was significantly lower in the DES group than in the BMS group: 445 of 4623 (9.6%) lesions versus 661 of 3536 (18.7%) lesions (relative risk 1.94 for the BMS group versus the DES group; $P < 0.01$; Fig. 1). Similarly, the rate of TLR was also significantly lower in the DES group than in the BMS group: 327 of 4623 (7.1%) lesions versus 472 of 3536 (13.6%) lesions (relative risk 1.46 for the BMS group versus the DES group; $P < 0.01$; Fig. 1). The long-term cumulative frequency of MACE in patients with ACS was similar in the BMS and DES groups: 83/1702 (4.9%) and 26/719 (3.6%) patients, respectively.

TABLE 2:
In-hospital and long-term cumulative major adverse cardiovascular events (MACE) in patients treated with a bare metal stent (BMS) or drug-eluting stent (DES) for coronary artery disease

Variable	BMS ($n = 2934$)	DES ($n = 3805$)	Statistical significance
No. of lesions treated by PCI	3536	4623	
In-hospital MACE[a]			$P < 0.0001$
Death, *n* (%)	40 (1.4)	9 (0.2)	$P < 0.0001$
Acute coronary syndrome	12 (0.4)	13 (0.3)	NS
Long-term cumulative MACE[b]			NS
Death, *n* (%)	39 (1.3)	24 (0.6)	NS
Acute coronary syndrome, *n* (%)	20 (0.7)	26 (0.7)	NS
TLR (% of total lesions)	472 (13.3)	327 (7.1)	NS

[a]In-hospital data refer to an interval of up to 30 days after the PCI procedure.
[b]Long-term data refer to the interval from 1 month to 1 year after percutaneous coronary intervention (PCI).
TLR, target lesion revascularization; NS, not statistically significant, $P > 0.05$.

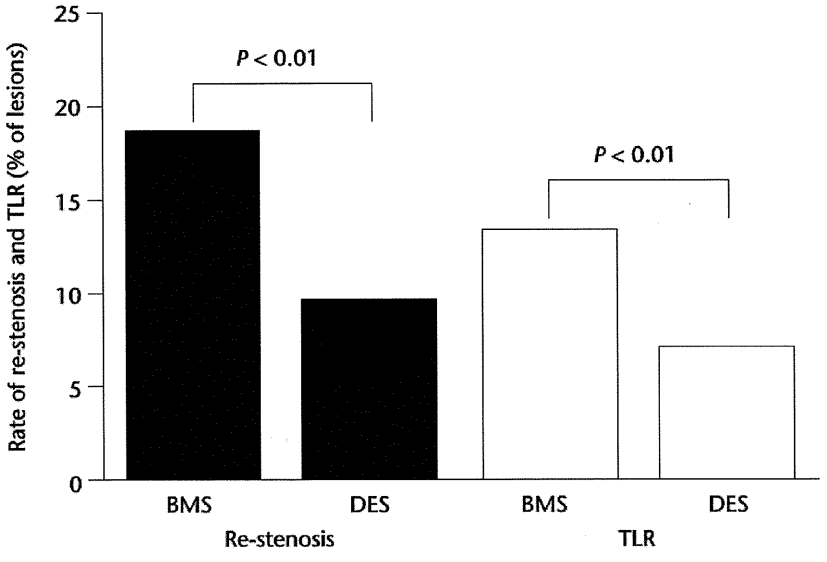

FIGURE 1: Rates of re-stenosis and target lesion revascularization (TLR) in patients treated with a bare metal stent (BMS) or a drug-eluting stent (DES) for coronary artery disease, determined on angiography at follow-up (mean ± SD follow-up interval 7.3 ± 4.9 months)

Subgroup analysis of re-stenosis

The overall in-stent re-stenosis rate was significantly ($P < 0.05$) greater in patients with DM (553/3070 patients; 18.0%) than in patients without DM (587/3669 patients; 16.0%). There was, however, no statistically significant effect of DM on the re-stenosis rate in the DES group (182/1899 patients [9.6%] with DM compared with 181/1906 patients without DM [9.5%]) whereas DM did have a statistically significant effect in the BMS group (249/1171 patients [21.3%] with DM compared with 301/1763 patients without DM [17.1%]; $P < 0.01$) (Fig. 2). There was no significant effect of other coronary risk factors with regard to the occurrence of re-stenosis.

Event-free survival analysis

Evaluation of event-free survival after stenting was examined in the BMS and DES groups by Kaplan–Meier analysis (Fig. 3). In one- and two-vessel disease, event-free survival decreased until about 200 and 300 days after stenting in patients treated with BMS and DES, respectively, and was significantly higher in the DES group than in the BMS group ($P < 0.001$). In three-vessel disease, event-free survival was also higher in the DES group than in the BMS group ($P < 0.001$) and the pattern of the Kaplan–Meier survival curves was similar to that of one- and two-vessel disease. In terms of patients fitted with a DES, event-free survival did not differ significantly between patients with one- or two-vessel disease and those with three-vessel disease, however, among patients treated with a BMS the long-term outcome of three-vessel disease was significantly worse than that of one- or two-vessel disease ($P < 0.001$). Event-free survival also decreased until 200 and 300 days after stenting of patients with LMCA disease in the BMS and DES groups, respectively, but the eventual survival rate did not differ significantly between these two groups.

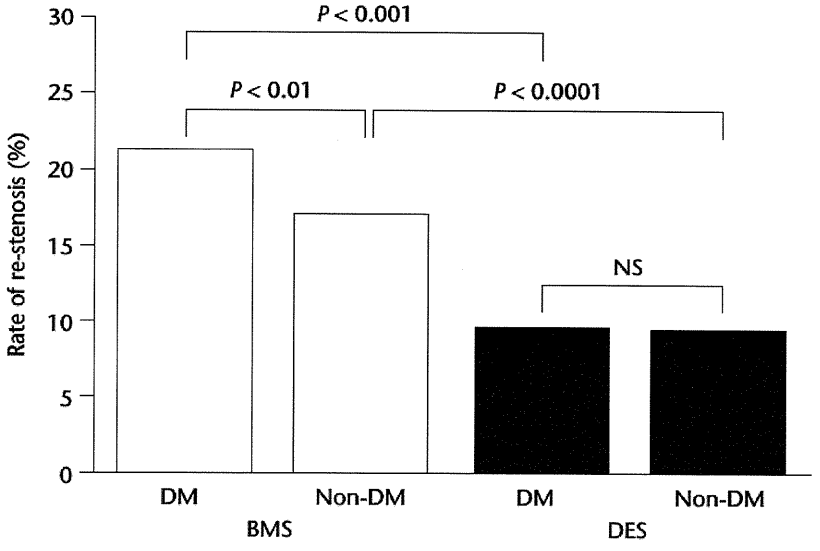

FIGURE 2: Re-stenosis rate 3 years after treatment with a bare metal stent (BMS) or a drug-eluting stent (DES) for coronary artery disease in patients with and without diabetes mellitus (DM) (NS, not statistically significant, $P > 0.05$)

Among patients with LMCA disease, event-free survival was significantly higher in those with non-bifurcation lesions (76/82 patients; 92.7%) than in those with bifurcation lesions (124/155 patients; 80.0%) ($P = 0.0433$). The outcome of LMCA lesions treated with a BMS or DES was worse than that of non-LMCA lesions and survival with

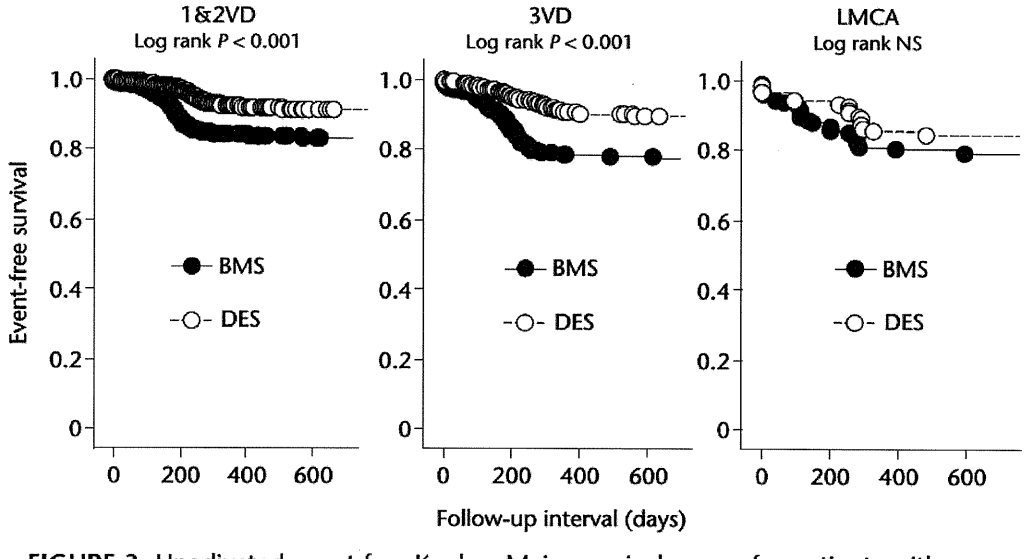

FIGURE 3: Unadjusted event-free Kaplan–Meier survival curves for patients with one- or two-vessel coronary artery disease (1&2VD), three-vessel disease (3VD) and left main coronary artery (LMCA) disease treated with a bare metal stent (BMS) or drug-eluting stent (DES) (NS, not statistically significant, $P > 0.05$)

a DES was superior to that with a BMS in patients with non-LMCA lesions (data not shown).

Discussion

The present study revealed that PCI in a real-world population was safe and feasible, with an angiographic procedural success rate of 98.2%, and the BMS and DES treatments were associated with low rates of MACE. Although the in-hospital MACE rate in the BMS group was significantly ($P < 0.0001$) higher than that in the DES group, this was considered to be because of the significantly higher incidence of patients with ACS who were treated with a BMS. There was no significant difference in MACE between the two groups when comparison was restricted only to patients showing ACS after stenting.

Implantation of a DES could reduce the risk of TLR by 40%, although it might also carry a minor risk of stent thrombosis and myocardial infarction within 2.7 years compared with BMS implantation.[10,11] In the present study, the relative risk of TLR following BMS implantation was 1.46 that of DES, however there were no differences between DES and BMS in the long-term risks of MACE (death, myocardial infarction or unstable angina associated with stent thrombosis). This may be explained by the fact that intravascular ultrasound and continuous dual antiplatelet therapy were frequently used.

It has been shown that DM is one of the most substantial risk factors for re-stenosis after stent implantation, with odds ratios of 1.9 – 2.5.[12] In the present study, using a DES led to a decrease in the rate of TLR compared with using a BMS, particularly in patients with DM. This result was consistent with a previous study in which TLR rates associated with a DES, during 4 years of follow-up, were 9.7% and 8.7% for patients with and without DM, respectively, and rates associated with a BMS were 22.4% and 16.4%, respectively.[13] Re-stenotic intimal hyperplasia in patients with DM may differ from that in patients without DM in terms of cellular aspects.[14,15] For example, diabetic vascular smooth muscle cells have been shown to exhibit increased rates of proliferation, leading to luminal narrowing.[14] A polymer coating, that releases anti-inflammatory and antiproliferative agents, is used in DES[15] and this may effectively prevent intimal proliferation in patients with or without DM.[16] We have reported previously that the use of a DES could suppress out-stent plaque progression, which was closely related to the progression of intimal hyperplasia[17] and this effect may be particularly relevant in the presence of DM.

The late outcome of one- and two-vessel disease, three-vessel disease and LMCA disease after DES and BMS implantation was evaluated in the present study. Event-free survival did not differ significantly between patients with one- or two-vessel disease and those with three-vessel coronary disease treated with a DES however, among patients treated with a BMS, the long-term outcome of three-vessel disease was worse than that of one- or two-vessel disease, probably because multivessel disease is often associated with multiple coronary risk factors.[18]

The outcome of LMCA lesions treated with a BMS or DES was worse than that of non-LMCA lesions. Although the eventual survival rate was not significantly different between the BMS and DES groups in LMCA disease, survival in patients fitted with a DES was superior to those with BMS in patients with non-LMCA lesions. Differences were particularly notable in bifurcation lesions. It is commonly thought that stenting for bifurcation lesions is associated with a high re-stenosis rate and this might have a

considerable impact on clinical survival.[19] We consider, therefore, that LMCA lesions should not be treated by DES implantation alone but additionally with interventions such as coronary artery bypass grafting, or by combining PCI with bypass surgery.

The present study had several limitations. First, because it was not randomized, the results might have been influenced by potential biases, however a relatively large number of patients (> 5000) were examined which may have minimized the effect of this limitation. Secondly, access to all information about the patients' medications, except for the antiplatelet agents used, was not available. This may have had some influence on the results, particularly regarding the long-term outcome. Indeed, several studies have reported different conclusions, suggesting superiority of the DES over the BMS in LMCA lesions.[20 – 23] Further large prospective trials, in which the effects of several coronary risk factors and lesion characteristics, especially LMCA lesions, are considered, may demonstrate differences between DES and BMS in severe coronary lesions, including those of the LMCA.

This evaluation of the clinical outcomes treated with stents in a real-world population of patients with coronary artery disease in Japan showed that the use of a DES dramatically decreased the rate of re-stenosis compared with the use of a BMS, particularly in patients with DM. However, very late re-stenosis was observed in a few cases treated with a DES, probably because of delayed healing of the stenting lesion. There was no statistically significant difference in event-free survival after stenting of patients with LMCA disease between the BMS and DES groups. We suggest careful treatment after using DES for severe coronary disease, including LMCA lesions, in patients with DM.

Appendix

The following hospitals in Japan, are affiliated with Kanazawa University Hospital: Kanazawa Cardiovascular Hospital, Fukui Cardiovascular Centre, Maizuru Kyousai Hospital, Ishikawa Prefectural Central Hospital, Toyama Red Cross Hospital, Yokohama Sakae Kyousai Hospital, Takaoka City Hospital, Komatsu Municipal Hospital, Fukui Prefectural Hospital, Koseiren Takaoka Hospital, Kaga Municipal Hospital, Houju Memorial Hospital, Saiseikai Kanazawa Hospital, Kanazawa Social Insurance Hospital, KKR Hokuriku Hospital.

Conflicts of interest

The authors had no conflicts of interest to declare in relation to this article.

• Received for publication 2 November 2010 • Accepted subject to revision 18 November 2011
• Revised accepted 2 April 2010

References

1 Favaloro RG: Saphenous vein autograft replacement of severe segmental coronary artery occlusion: operative technique. *Ann Thorac Surg* 1968; **5:** 334 – 339.
2 Gruntzig A: Transluminal dilatation of coronary-artery stenosis. *Lancet* 1978; **i:** 263.
3 Palmaz JC: Balloon-expandable intravascular stent. *AJR Am J Roentgenol* 1988; **150:** 1263 – 1269.
4 Serruys PW, de Jaegere P, Kiemeneij F, *et al* for the Benestent Study Group: A comparison of balloon-expandable-stent implantation with balloon angioplasty in patients with coronary artery disease. *N Engl J Med* 1994; **331:** 489 – 495.
5 Ormiston JA, Dixon SR, Webster MW, *et al*: Stent longitudinal flexibility: a comparison of 13 stent designs before and after balloon expansion. *Catheter Cardiovasc Interv* 2000; **50:**

120 – 124.
6 Niles NW, McGrath PD, Malenka D, *et al* for the Northern New England Cardiovascular Disease Study Group: Survival of patients with diabetes and multivessel coronary artery disease after surgical or percutaneous coronary revascularization: results of a large regional prospective study. *J Am Coll Cardiol* 2001; **37:** 1008 – 1015.
7 Kimura T, Morimoto T, Furukawa Y, *et al*: Long-term outcomes of coronary-artery bypass graft surgery versus percutaneous coronary intervention for multivessel coronary artery disease in the bare-metal stent era. *Circulation* 2008; **118(14 suppl):** S199 – S209.
8 Jensen LO, Tilsted HH, Thayssen P, *et al*: Paclitaxel and sirolimus eluting stents versus bare metal stents: long-term risk of stent thrombosis and other outcomes. From the Western Denmark Heart Registry. *EuroIntervention* 2010; **5:** 898 – 905.
9 Park DW, Kim YH, Yun SC, *et al*: Long-term outcomes after stenting versus coronary artery bypass grafting for unprotected left main coronary artery disease: 10-year results of bare-metal stents and 5-year results of drug-eluting stents from the ASAN–MAIN (ASAN Medical Center–Left MAIN Revascularization) Registry. *J Am Coll Cardiol* 2010; **56:** 1366 – 1375.
10 Auer J, Leitner A, Berent R, *et al*: Long-term outcomes following coronary drug-eluting- and bare-metal-stent implantation. *Atherosclerosis* 2010; **210:** 503 – 509.
11 Lagerqvist B, James SK, Stenestrand U, *et al*: Long-term outcomes with drug-eluting stents versus bare-metal stents in Sweden. *N Engl J Med* 2007; **356:** 1009 – 1019.
12 Airoldi F, Briguori C, Iakovou I, *et al*: Comparison of sirolimus versus paclitaxel eluting stents for treatment of coronary in-stent restenosis. *Am J Cardiol* 2006; **97:** 1182 – 1187.
13 Stettler C, Allemann S, Wandel S, *et al*: Drug eluting and bare metal stents in people with and without diabetes: collaborative network meta-analysis. *BMJ* 2008; **337:** a1331.
14 Moreno PR, Murcia AM, Palacios IF, *et al*: Coronary composition and macrophage infiltration in atherectomy specimens from patients with diabetes mellitus. *Circulation* 2000; **102:** 2180 – 2184.
15 Lexis CP, Rahel BM, Meeder JG, *et al*: The role of glucose lowering agents on restenosis after percutaneous coronary intervention in patients with diabetes mellitus. *Cardiovasc Diabetol* 2009; **8:** 41.
16 Airoldi F, Briguori C, Iakovou I, *et al*: Comparison of sirolimus versus paclitaxel eluting stents for treatment of coronary in-stent restenosis. *Am J Cardiol* 2006; **97:** 1182 – 1187.
17 Tada H, Kawashiri MA, Sakata K, *et al*: Impact of out-stent plaque volume on in-stent intimal hyperplasia: result from serial volumetric analysis with high-gain intravascular ultrasound. *Int J Cardiol* 2011; epub ahead of print.
18 Serruys PW, Morice MC, Kappetein AP, *et al*: Percutaneous coronary intervention versus coronary-artery bypass grafting for severe coronary artery disease. *N Engl J Med* 2009; **360:** 961 – 972.
19 Sheiban I, Sillano D, Biondi-Zoccai G, *et al*: Incidence and management of restenosis after treatment of unprotected left main disease with drug-eluting stents: 70 restenotic cases from a cohort of 718 patients: FAILS (Failure in Left Main Study). *J Am Coll Cardiol* 2009; **54:** 1131 – 1136.
20 Chieffo A, Stankovic G, Bonizzoni E, *et al*: Early and mid-term results of drug-eluting stent implantation in unprotected left main. *Circulation* 2005; **111:** 791 – 795.
21 Valgimigli M, van Mieghem AG, Ong ATL, *et al*: Short- and long-term clinical outcome after drug-eluting stent implantation for the percutaneous treatment of left main coronary artery disease: insights from the Rapamycin-Eluting and Taxus Stent Evaluated At Rotterdam Cardiology Hospital (RESEARCH and T-SEARCH) registries. *Circulation* 2005; **111:** 1383 – 1389.
22 Park SJ, Kim YH, Lee BK, *et al*: Sirolimus-eluting stent implantation for unprotected left main coronary artery stenosis: comparison with bare metal stent implantation. *J Am Coll Cardiol* 2005; **45:** 351 – 356.
23 Gao R, Xu B, Chen J, *et al*: Immediate and long-term outcomes of drug-eluting stent implantation for unprotected left main coronary artery disease: comparison with bare-metal stent implantation. *Am Heart J* 2008; **155:** 553 – 561.

Author's address for correspondence
Dr Katsuharu Uchiyama
Division of Cardiovascular Medicine, Kanazawa University Graduate School of Medicine,
Takara-Machi 13-1, Kanazawa 920-8640, Japan.
E-mail: angio@staff.kanazawa-u.ac.jp

Journal of Cardiology (2011) 57, 89–94

available at www.sciencedirect.com

ScienceDirect

journal homepage: www.elsevier.com/locate/jjcc

Original article

Impact of reduced left atrial functions on diagnosis of paroxysmal atrial fibrillation: Results from analysis of time-left atrial volume curve determined by two-dimensional speckle tracking

Mika Mori (MD)[a], Hideaki Kanzaki (MD)[b], Makoto Amaki (MD)[b], Takahiro Ohara (MD)[b], Takuya Hasegawa (MD)[b], Hiroyuki Takahama (MD)[b], Kazuhiko Hashimura (MD)[b], Tetsuo Konno (MD)[a], Kenshi Hayashi (MD)[a], Masakazu Yamagishi (MD, FJCC)[a,*], Masafumi Kitakaze (MD, FJCC)[b]

[a] *Division of Cardiovascular Medicine, Kanazawa University Graduate School of Medicine, 13-1 Takara-machi, Kanazawa, 920-8641 Ishikawa, Japan*
[b] *Division of Heart Failure, Cardiovascular Medicine, National Cerebral and Cardiovascular Center, Suita, Osaka, Japan*

Received 4 August 2010; accepted 11 August 2010
Available online 15 October 2010

KEYWORDS
Atrial fibrillation;
Echocardiography;
Speckle tracking method;
Reservoir function;
Booster function

Summary
Background: Atrial fibrillation is commonly associated with impaired reservoir and booster functions of the left atrium (LA). Recent advances in two-dimensional speckle tracking technique (2DST) enabled automatic analysis of the time-LA volume curve representing these functions. Our objective was to evaluate LA function in patients with or without paroxysmal atrial fibrillation (PAF) using 2DST.
Methods: We studied 111 patients (68 men, age 62 ± 16 years) with (n = 53) or without (n = 58) PAF. After constructing time-LA volume curves from the apical four and two chamber views (iE33, Philips with QLAB 6.0, Philips Medical Systems, Bothell, WA, USA), maximal LA volume (LAVmax), preatrial contraction LA volume (LAVpreA), and minimum LA volume (LAVmin) were obtained. Then, LA reservoir volume (ARV = LAVmax − LAVmin) and active emptying volume (AEV = LAVpreA − LAVmin) were calculated to determine ARV/LAVmax as reservoir function and AEV/LAVpreA as booster pump function.

* Corresponding author. Tel.: +81 6 76 265 2259; fax: +81 76 234 4210.
E-mail address: myamagi@med.kanazawa-u.ac.jp (M. Yamagishi).

0914-5087/$ – see front matter
doi:10.1016/j.jjcc.2010.08.006

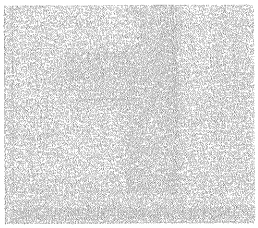

Results: PAF was associated with greater LAVmax than that in controls (80 ± 21 ml versus 65 ± 16 ml, $p < 0.001$) and with reduced reservoir and booster functions (ARV/LAVmax 46 ± 9% versus 52 ± 7%; AEV/LAVpreA 29 ± 10% versus 36 ± 6%, $p < 0.001$). Multivariate logistic analysis demonstrated that ARV/LAVmax and AEV/LAVpreA were closely associated with the existence of PAF.

Conclusion: These results demonstrate that the present 2DST enables determining LA reservoir and booster functions, providing insights into the diagnosis of PAF.

Introduction

It is well established that cardiogenic embolism could suddenly occlude the cerebral artery without the development of collateral circulation, thus resulting in large infarction associated with severe paralysis and/or consciousness disturbance. Actually, atrial fibrillation (AF) is the independent risk factor for cardiogenic stroke and relative risk increases up to 5 times in comparison with cases without AF [1]. There exists a strong correlation between left atrial (LA) volume and occurrence of AF [2], and an enlarged LA could be a predictive factor for the occurrence of stroke even without the evidence of AF [3]. This suggests that the diagnosis of possible occurrence of AF at the time of sinus rhythm is important for the prevention of cardiogenic stroke when considering that paroxysmal AF (PAF) has the same impact on the occurrence of stroke as persistent or chronic AF [4].

LA mechanical functions consist of three components at different stages of the cardiac cycle: active and passive LA enlargement, as a reservoir, associated with pulmonary inflow at the time of left ventricular systole to isovolumetric relaxation, conduit function during early ventricular diastole, and active systole to transfer blood, as a booster, during late ventricular diastole [5]. Although AF is a situation in which LA booster pump function is lost, this booster function as well as reservoir function could be impaired even in PAF [6–8].

Although three-dimensional echocardiography [9] and acoustic quantification (AQ) [10,11] have been used for the evaluation of these LA functions, they were somewhat complicated to obtain reliable results. Recent advances in two-dimensional speckle tracking technique (2DST) enabled analyzing time-LA volume curve [12]. In the present study, using 2DST we attempted to evaluate LA function in patients with or without PAF examining possible indices to diagnose PAF.

Methods

Study subjects

We studied a total of 111 patients (68 men, age 62 ± 16 years) including 53 patients with PAF which was documented by electrocardiogram (ECG) including conventional, ambulatory, and remote monitoring systems, and 58 patients who did not exhibit any cardiac abnormalities with sinus rhythm as controls. Exclusion criteria included the presence of significant valvular disease, intracardiac shunting, left ventricular (LV) systolic dysfunction defined as LV ejection fraction (EF) < 50%, hyperthyroidism, primary pulmonary hypertension, and respiratory disease. We also excluded patients who showed inadequate echocardiographic images. All the research protocols were approved by ethical committee and informed consent was obtained from all patients.

Patients' characteristics in the present study included age, sex, height, body weight, systolic blood pressure, diastolic blood pressure, heart rate, absence or presence of hypertension, diabetes mellitus, and dyslipidemia. Current drug treatments were also recorded. Hypertension was defined as systolic blood pressure ≥140 mm Hg and/or diastolic blood pressure ≥90 mm Hg. We also defined hypertension if patients already had anti-hypertensive medication. Diabetes mellitus was defined when diabetic patterns such as fasting plasma glucose levels ≥126 mg/dl, 2-h plasma glucose levels by 75 g oral glucose tolerance test ≥200 mg/dl, or casual plasma glucose levels ≥200 mg/dl were observed on at least two occasions. Patients who exhibited diabetic pattern at least once and diabetic symptoms or retinopathy or HbA1c ≥6.5% were also defined as having diabetes mellitus. Dyslipidemia was defined as low-density lipoprotein cholesterol ≥140 mg/dl and/or high-density lipoprotein cholesterol <40 mg/dl or triglyceride ≥150 mg/dl.

Echocardiography

All echocardiographic examinations were performed using an iE33 system and an S5-1 broadband phased array transducer (Philips Medical Systems, Bothell, WA, USA). At first, LA dimension was determined by M-mode from the parasternal long-axis view. Then, thickness of interventricular septum and posterior wall, LV end-diastolic and end-systolic dimensions, and LVEF were determined in accordance with the guideline of the American Society of Echocardiography [13].

Using pulsed Doppler method, transmitral flow velocity such as *E* and *A* waves, and deceleration time of *E* wave (E-DcT) were measured. Finally, from the apical four chamber view, the average of peak early and late diastolic mitral annular velocity (e' and a') between medial and lateral sides was determined by pulsed tissue Doppler method. E/e' was then calculated as an index of LV end-diastolic pressure.

Analysis of time-left atrial volume curve

We analyzed echocardiographic data using commercially available QLAB 6.0 software (Philips Medical Systems). Briefly, when we set three points at the septal and lateral sides of mitral annulus and roof of LA in the apical four chamber view at LV end-diastole defined as R wave on the ECG, software automatically drew a region of interest (ROI) like

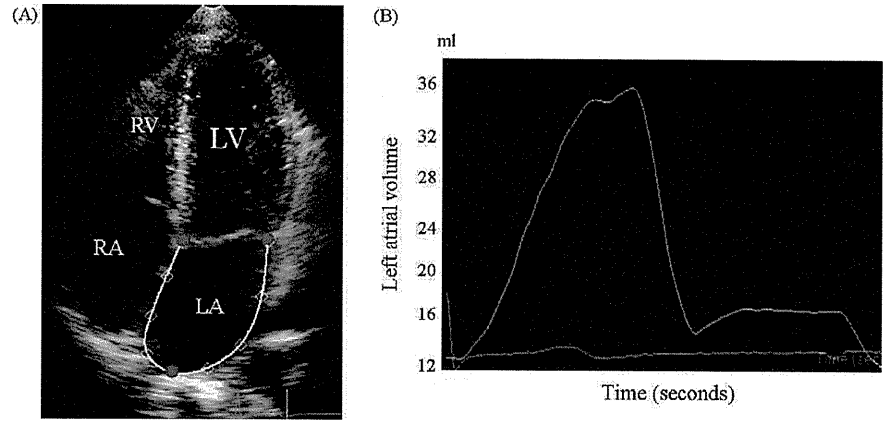

Figure 1 (A) Two-dimensional speckle tracking in the left atrial wall. Red circles represent initially set regions of interest (ROIs). White squares represent ROIs which are automatically added. White lines represent complementary lines between each ROI. (B) Representative left atrial volume curve during a cardiac cycle. LA, left atrium; LV, left ventricle; RA, right atrium; RV, right ventricle. (For interpretation of the references to color in this figure legend, the reader is referred to the web version of the article.)

a horseshoe shape at the inner side of LA wall, the septal and lateral sides of mitral annulus, and the top of LA. In the present study, we changed the setup of the number of points to drag and modify the shape of ROI to three at each wall (total 9 points). After manually adjusting the ROI, LA volume was calculated by Simpson's rule using spline interpolation frame by frame throughout the cardiac cycle to derive a time-LA volume curve (Fig. 1). Then, a time-LA volume curve was also obtained from the apical two-chamber view as well.

Three types of LA volume were determined: maximal LA volume (LAVmax) at the LV end-systolic phase just before mitral valve opening, preatrial contraction LA volume (LAVpreA) at the beginning of P-wave on the ECG, and minimal LA volume (LAVmin) at the LV end-diastolic phase just after mitral valve closure (Fig. 2). We calculated LA reservoir volume (ARV = LAVmax − LAVmin) and active emptying volume (AEV = LAVpreA − LAVmin) and defined ARV/LAVmax as a reservoir index and AEV/LAVpreA as a booster pump index according to the published reports [5,11].

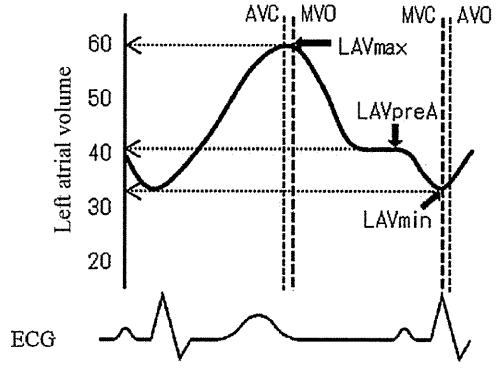

Figure 2 Schematic representations of time-left atrial volume curve and measurement of left atrial volume. AVC, aortic valve closure; AVO, aortic valve opening; ECG, electrocardiogram; LAVmax, maximum left atrial volume; LAVmin, minimum left atrial volume; LAVpreA, preatrial contraction left atrial volume; MVC, mitral valve closure; MVO, mitral valve opening.

Statistical analysis

Data are shown as mean ± SD. An analysis of variance (ANOVA) was performed to test for statistically significant differences between two unpaired mean values, and categorical data and percentage frequencies were analyzed by the chi-square test. PAF-associated factors were examined by multivariate logistic analysis. We used SPSS 16.0J for Windows for analysis (SPSS Inc, Chicago, IL, USA). Statistical significance was considered when $p < 0.05$.

Twenty subjects were randomly selected and analyzed to assess reproducibility. The inter- and intraobserver variability was 5.7 ± 3.2% and 6.2 ± 3.9% for LAVmax, 7.6 ± 5.0% and 5.8 ± 4.9% for LAVpreA, 7.0 ± 4.6% and 7.7 ± 3.3% for LAVmin.

Results

Patients' backgrounds

Age and systolic and diastolic blood pressures were higher in PAF than those in controls, although heart rate was lower in controls. There were no differences in sex and BMI between two groups. Also there were no differences in incidence of hypertension, diabetes, and dyslipidemia. Although the use of angiotensin-converting enzyme inhibitors and/or angiotensin II receptor blockers was not different in both groups, the use of β-blockers was greater in PAF than that in non-PAF (Table 1).

In echocardiographic parameters, LA dimension and *E* wave velocity were greater in PAF, although E-DcT was shorter in PAF. *E*/*e*′ was greater in PAF because of significantly decreased *e*′ and increased *E*. There were no

Table 1 Patients' background.

Parameters	Control group ($n=58$)	PAF group ($n=53$)	p-value
Age, years	58 ± 17	66 ± 13	0.002
Male, %	57	66	NS
Body mass index, kg/m^2	23 ± 2.8	23 ± 2.4	NS
Systolic blood pressure, mm Hg	132 ± 18	139 ± 18	0.023
Diastolic blood pressure, mm Hg	76 ± 12	80 ± 10	0.026
Heart rate, beats/min	65 ± 10	60 ± 8	0.013
Hypertension, %	57	58	NS
Diabetes mellitus, %	16	10	NS
Dyslipidemia, %	21	16	NS
Drug treatment			
ACEI or ARB, %	11	9	NS
Beta-blocker, %	3	12	0.016

Data are mean ± SD.
ACEI, angiotensin-converting enzyme inhibitor; ARB, angiotensin II receptor blocker; PAF, paroxysmal atrial fibrillation.

significant differences in LV dimensions, LV fractional shortening, LV wall thickness, *A* wave velocity, *E*/*A* and *a*′ between the two groups (Table 2).

Left atrial volume and indices of left atrial function

All data regarding LA volume and functional indices are summarized in Table 3. LAVmax, LAVpreA, and LAVmin were greater in PAF than those in controls ($p<0.05$). As for LA functions, both ARV/LAVmax as the index for reservoir function and AEV/LAVpreA as the index for booster pump function were lower in PAF in comparison with those in controls ($p<0.05$).

Determining factors for PAF

We determined the diagnostic value of the LA volume and function in predicting PAF using logistic analysis. After adjusting for age, sex, and presence or absence of hypertension, increases in LAVmax, and decreases in ARV/LAVmax and AEV/LAVpreA were associated with the existence of PAF (Table 4).

Table 2 Echocardiographic parameters.

Parameters	Control group	PAF group	p-value
LA dimension, mm	37 ± 5	40 ± 6	0.002
LVDd, mm	45 ± 3	47 ± 5	NS
LVDs, mm	28 ± 3	29 ± 4	NS
LVFS, %	37 ± 6	38 ± 5	NS
IVS, mm	9 ± 1	9 ± 1	NS
PW, mm	9 ± 1	9 ± 1	NS
E velocity, cm/s	63 ± 18	71 ± 16	0.017
A velocity, cm/s	67 ± 20	73 ± 20	NS
E/*A*	1.1 ± 0.6	1.1 ± 0.5	NS
E-DcT, ms	230 ± 60	209 ± 44	0.037
e′, cm/s	8.4 ± 3.5	7.1 ± 2.0	0.017
a′, cm/s	9.8 ± 1.6	8.9 ± 2.2	NS
E/*e*′	8.3 ± 3.4	10.5 ± 3.6	0.001

Data are mean ± SD. *a*′, peak late diastolic mitral annular velocity; *e*′, peak early diastolic mitral annular velocity; E-DcT, *E* wave deceleration time; IVS, interventricular wall thickness; LA, left atrium; LVDd, left ventricular end-diastolic dimension; LVDs, left ventricular end-systolic dimension; LVFS, left ventricular fractional shortening; PAF, paroxysmal atrial fibrillation; PW, posterior wall thickness.

Table 3 Left atrial volume and functional indices by two-dimensional speckle tracking method.

Parameters	Control group	PAF group	p-value
LAVmax, ml	65 ± 16	80 ± 21	0.002
LAVpreA, ml	49 ± 15	61 ± 19	0.037
LAVmin, ml	31 ± 10	44 ± 16	0.004
ARV/LAVmax, %	52.2 ± 7.1	46.3 ± 9.3	0.001
AEV/LAVpreA, %	35.6 ± 5.8	28.6 ± 9.6	0.001

Data are mean ± SD.
AEV, active emptying volume = LAVpreA − LAVmin; ARV, atrial reservoir volume = LAVmax − LAVmin; LAVmax, maximum left atrial volume; LAVpreA, preatrial contraction left atrial volume; LAVmin, minimum left atrial volume; PAF, paroxysmal atrial fibrillation.

Table 4 Adjusted odds ratio for paroxysmal atrial fibrillation.

	Odds ratio (95%CI)	p-value
LAVmax, ml	1.534 (1.186–1.983) (/10 ml increase)	0.001
LAVmax/BSA, ml/m^2	2.135 (1.335–3.414) (10 ml/m^2 increase)	0.002
ARV/LAVmax, %	1.457 (1.117–1.900) (5% decline)	0.005
AEV/LAVpreA, %	1.835 (1.334–2.523) (5% decline)	<0.001

Data are mean ± SD.
AEV, active emptying volume = LAVpreA − LAVmin; ARV, atrial reservoir volume = LAVmax − LAVmin; BSA, body surface area; CI, confidence interval; LAVmax, maximal left atrial volume; LAVpreA, preatrial contraction left atrial volume.

Discussion

Occurrence of paroxysmal atrial fibrillation and left atrial function

Enlargement of LA is known to be related to aging, hypertension, and LV diastolic dysfunction, and is an independent factor for occurrence of AF [14–17]. In the present study, LAVmax was found to be an independently associated factor for paroxysmal AF even after adjusting for other factors such as aging, sex, and presence of hypertension. On the other hand, enlargement of LA reflects the duration of AF periods, because AF itself can enhance LA remodeling [17]. In addition to LAVmax, LAVpreA and LAVmin were found to be greater in PAF than those in controls. Fatema et al. [18] reported that not only LAVmax but also LAVmin were independent predicting factors for AF, and, under these conditions, LAVmin might be better than LAVmax in terms of predicting value for AF. However, as pointed out in a previous [18] and in our study, reproducibility for measurement of LAVmin was found not enough to use for clinical practice.

LA reservoir function is considered as a combination of active LA dilation and passive dilation due to declining of mitral annulus associated with LV contraction. Abhayaratna et al. [19] demonstrated that the probability of occurrence of AF would increase by 9 times in patients with LAVmax/BSA $\geq$38 ml/m^2 and ARV/LAVmax $\leq$49% in comparison with patients with LAVmax/BSA <38 ml/m^2 and ARV/LAVmax >49%. This suggests that in addition to LA volume, evaluation of LA function should be done to predict the occurrence of AF.

LA reservoir function can represent LA diastolic function and can be evaluated by the strain-rate imaging method. Wang et al. [7] reported that hypertensive patients with PAF exhibited lower LA strain rate than those without PAF, suggesting that LA reservoir function may reflect the progression of atrial remodeling because the recurrence rate of AF after catheter ablation was higher in patients with low strain rates of left ventricle and atrium [20]. The present ARV/LAVmax actually represented LA reservoir function and was reduced in PAF, suggesting that this reflected the impaired reservoir function. From the time-LA volume curve obtained by 2DST, we can obtain first derivation curve which also represents the strain rate of the whole left atrium. Unfortunately, it was somewhat difficult to obtain reliable data regarding peak value of this index from the present study because of the presence of artifact due to noise. However, it will be possible to overcome these difficulties if adequate frame rates and adequate noise filters are chosen.

LA booster pump function can increase in accordance with increase in LA preload until disruption of Frank–Starling law and contribute to maintaining cardiac output [5,21]. However, this function may decrease in accordance with progression of LA remodeling associated with AF [22]. Cui et al. [8] reported that AEV/LAVpreA which was determined by AQ method was significantly lower in PAF with hypertension than that without PAF. As for other indices for assessment of LA function, *A* wave velocity [23] and tissue Doppler-derived *a'* [24] were used. In the present study, there were significant differences in AEV/LAVpreA despite the absence of significant differences in *A* wave and *a'*, suggesting that AEV/LAVpresA determined by 2DST is more sensitive in the evaluation of LA remodeling in clinical settings.

Two-dimensional speckle tracking method

Previously, measurement of LA volume for time-LA volume curve analysis has been performed by the AQ method [10,11]. However, it is somewhat difficult to exclude the presence of pulmonary vein and/or LA appendage, thus resulting in inadequate quantification of LA volume, because automatic determination of blood-tissue border by the AQ method is performed within an oval ROI [25]. In contrast, in the 2DST method we can set an ROI freely and adjust it on looking at the situation of tracking. Therefore, one might speculate that measurement might be more accurate in 2DST than that in AQ.

Although LA volume determined by three-dimensional echocardiography coincided well with that determined by magnetic resonance imaging [9], this procedure requires some technical experience and time. We previously reported that LA volume measured by 2DST coincided well with that by real-time three-dimensional echocardiography [26]. Ogawa et al. [27] demonstrated that time to create time-LA volume curve by 2DST was much shorter than that by manual examination. Okamatsu et al. [12] studied 140 subjects by 2DST on LA reservoir and booster functions and demonstrated impaired reservoir and enhanced booster functions were observed in old people. This suggests the higher sensitivity of the present study to detect the LA reservoir and booster functions than previous methods in clinical settings, although we did not compare each methodology.

Study limitations

There remain several limitations in the present study. First, we examined patients without evidenced PAF as controls. However, we could not exclude the possibility that these controls might have an asymptomatic AF. Also it was difficult to determine the adequate cutoff value in each index because of the limited number of subjects. Second, the present study was not longitudinal but a transverse study and, thus, it is difficult to predict the occurrence of AF and/or thromboembolism. To complete this issue, additional follow-up study will be required to determine absolute value of these indices for predicting the occurrence of clinical events.

Conclusions

The present study demonstrates that using 2DST LA reservoir and booster functions in PAF are impaired in comparison with controls. We suggest that the indices obtained by the present method provide alternative objective findings for predicting possible occurrence of PAF.

Acknowledgments

A part of this work was presented at the 57th Annual Scientific Sessions, Japanese College of Cardiology, 2009, Sapporo, Japan.

References

[1] Wolf PA, Abbott RD, Kannel WB. Atrial fibrillation as an independent risk factor for stroke: the Framingham Study. Stroke 1991;22:983–8.

[2] Tsang TS, Barnes ME, Bailey KR, Leibson CL, Montgomery SC, Takemoto Y, Diamond PM, Marra MA, Gersh BJ, Wiebers DO, Petty GW, Seward JB. Left atrial volume: important risk marker of incident atrial fibrillation in 1655 older men and women. Mayo Clin Proc 2001;76:467–75.

[3] Barnes ME, Miyasaka Y, Seward JB, Gersh BJ, Rosales AG, Bailey KR, Petty GW, Wiebers DO, Tsang TS. Left atrial volume in the prediction of first ischemic stroke in an elderly cohort without atrial fibrillation. Mayo Clin Proc 2004;79:1008–14.

[4] Hohnloser SH, Pajitnev D, Pogue J, Healey JS, Pfeffer MA, Yusuf S, Connolly SJ, ACTIVE W Investigators. Incidence of stroke in paroxysmal versus sustained atrial fibrillation in patients taking oral anticoagulation or combined antiplatelet therapy: an ACTIVE W Substudy. J Am Coll Cardiol 2007;50:2156–61.

[5] Zhang G, Yasumura Y, Uematsu M, Nakatani S, Nagaya N, Miyatake K, Yamagishi M. Echocardiographic determination of left atrial function and its application for assessment of mitral flow velocity pattern. Int J Cardiol 1999;72:19–25.

[6] Barbier P, Alioto G, Guazzi MD. Left atrial function and ventricular filling in hypertensive patients with paroxysmal atrial fibrillation. J Am Coll Cardiol 1994;24:165–70.

[7] Wang Z, Tan H, Zhong M, Jiang G, Zhang Y, Zhang W. Strain rate imaging for noninvasive functional quantification of the left atrium in hypertensive patients with paroxysmal atrial fibrillation. Cardiology 2008;109:15–24.

[8] Cui Q, Wang H, Zhang W, Wang H, Sun X, Zhang Y, Yang H. Enhanced left atrial reservoir, increased conduit, and weakened booster pump function in hypertensive patients with paroxysmal atrial fibrillation. Hypertens Res 2008;31:395–400.

[9] Poutanen T, Ikonen A, Vainio P, Jokinen E, Tikanoja T. Left atrial volume assessed by transthoracic three dimensional echocardiography and magnetic resonance imaging: dynamic changes during the heart cycle in children. Heart 2000;83:537–42.

[10] Zhang GC, Tsukada T, Nakatani S, Uematsu M, Yasumura Y, Tanaka N, Masuda Y, Miyatake K, Yamagishi M. Comparison of automatic boundary detection and manual tracing technique in echocardiographic determination of left atrial volume. Jpn Circ J 1998;62:755–9.

[11] Spencer KT, Mor-Avi V, Gorcsan III J, DeMaria AN, Kimball TR, Monaghan MJ, Perez JE, Weinert L, Bednarz J, Edelman K, Kwan OL, Glascock B, Hancock J, Baumann C, Lang RM. Effects of aging on left atrial reservoir, conduit, and booster pump function: a multi-institution acoustic quantification study. Heart 2001;85:272–7.

[12] Okamatsu K, Takeuchi M, Nakai H, Nishikage T, Salgo IS, Husson S, Otsuji Y, Lang RM. Effects of aging on left atrial function assessed by two-dimensional speckle tracking echocardiography. J Am Soc Echocardiogr 2009;22:70–5.

[13] Lang RM, Bierig M, Devereux RB, Flachskampf FA, Foster E, Pellikka PA, Picard MH, Roman MJ, Seward J, Shanewise JS, Solomon SD, Spencer KT, Sutton MS, Stewart WJ. Recommendations for chamber quantification: a report from the American Society of Echocardiography's Guidelines and Standards Committee and the Chamber Quantification Writing Group, developed in conjunction with the European Association of Echocardiography, a branch of the European Society of Cardiology. J Am Soc Echocardiogr 2005;18:1440–63.

[14] Casaclang-Verzosa G, Gersh BJ, Tsang TS. Structural and functional remodeling of the left atrium: clinical and therapeutic implications for atrial fibrillation. J Am Coll Cardiol 2008;51:1–11.

[15] Psaty BM, Manolio TA, Kuller LH, Kronmal RA, Cushman M, Fried LP, White R, Furberg CD, Rautaharju PM. Incidence of and risk factors for atrial fibrillation in older adults. Circulation 1997;96:2455–61.

[16] Healey JS, Connolly SJ. Atrial fibrillation: hypertension as a causative agent, risk factor for complications, and potential therapeutic target. Am J Cardiol 2003;91:9G–14G.

[17] Thamilarasan M, Klein AL. Factors relating to left atrial enlargement in atrial fibrillation: ''chicken or the egg'' hypothesis. Am Heart J 1999;137:381–3.

[18] Fatema K, Barnes ME, Bailey KR, Abhayaratna WP, Cha S, Seward JB, Tsang TS. Minimum vs. maximum left atrial volume for prediction of first atrial fibrillation or flutter in an elderly cohort: a prospective study. Eur J Echocardiogr 2009;10:282–6.

[19] Abhayaratna WP, Fatema K, Barnes ME, Seward JB, Gersh BJ, Bailey KR, Casaclang-Verzosa G, Tsang TS. Left atrial reservoir function as a potent marker for first atrial fibrillation or flutter in persons > or = 65 years of age. Am J Cardiol 2008;101:1626–9.

[20] Schneider C, Malisius R, Krause K, Lampe F, Bahlmann E, Boczor S, Antz M, Ernst S, Kuck KH. Strain rate imaging for functional quantification of the left atrium: atrial deformation predicts the maintenance of sinus rhythm after catheter ablation of atrial fibrillation. Eur Heart J 2008;29:1397–409.

[21] Anwar AM, Geleijnse ML, Soliman OI, Nemes A, ten Cate FJ. Left atrial Frank–Starling law assessed by real-time, three-dimensional echocardiographic left atrial volume changes. Heart 2007;93:1393–7.

[22] Toh N, Kanzaki H, Nakatani S, Ohara T, Kim J, Kusano KF, Hashimura K, Ohe T, Ito H, Kitakaze M. Left atrial volume combined with atrial pump function identifies hypertensive patients with a history of paroxysmal atrial fibrillation. Hypertension 2010;55:1150–6.

[23] Manning WJ, Silverman DI, Katz SE, Riley MF, Come PC, Doherty RM, Munson JT, Douglas PS. Impaired left atrial mechanical function after cardioversion: relation to the duration of atrial fibrillation. J Am Coll Cardiol 1994;23:1535–40.

[24] Nagueh SF, Sun H, Kopelen HA, Middleton KJ, Khoury DS. Hemodynamic determinants of the mitral annulus diastolic velocities by tissue Doppler. J Am Coll Cardiol 2001;37:278–85.

[25] Tsujita-Kuroda Y, Zhang G, Sumita Y, Hirooka K, Hanatani A, Nakatani S, Yasumura Y, Miyatake K, Yamagishi M. Validity and reproducibility of echocardiographic measurement of left ventricular ejection fraction by acoustic quantification with tissue harmonic imaging technique. J Am Soc Echocardiogr 2000;13:300–5.

[26] Mori M, Hasegawa T, Kanzaki H, Maeda M, Yoshida A, Watanabe M, Harada K, Takahama H, Amaki M, Ohara T, Hashimura K, Kitakaze M. Evaluation of left atrial function in paroxysmal atrial fibrillation: application of two-dimensional speckle tracking method for analysis of left atrial volume curve. J Cardiol 2009;4(Suppl. I):220.

[27] Ogawa K, Hozumi T, Sugioka K, Iwata S, Otsuka R, Takagi Y, Yoshitani H, Yoshiyama M, Yoshikawa J. Automated assessment of left atrial function from time-left atrial volume curves using a novel speckle tracking imaging method. J Am Soc Echocardiogr 2009;22:63–9.

Journal of Molecular and Cellular Cardiology 50 (2011) 50–57

Contents lists available at ScienceDirect

Journal of Molecular and Cellular Cardiology

journal homepage: www.elsevier.com/locate/yjmcc

Original article

A *KCR1* variant implicated in susceptibility to the long QT syndrome

Kenshi Hayashi [a,*], Noboru Fujino [a], Hidekazu Ino [a], Katsuharu Uchiyama [a], Kenji Sakata [a], Tetsuo Konno [a], Eiichi Masuta [a], Akira Funada [a], Yuichiro Sakamoto [a], Toshinari Tsubokawa [a], Akihiko Hodatsu [a], Toshihiko Yasuda [b], Honin Kanaya [b], Min Young Kim [c], Sabina Kupershmidt [c], Haruhiro Higashida [d], Masakazu Yamagishi [a]

[a] *Division of Cardiovascular Medicine, Kanazawa University Graduate School of Medical Science, Kanazawa, Ishikawa, Japan*
[b] *Ishikawa Prefectural Central Hospital, Kanazawa, Ishikawa, Japan*
[c] *Anesthesiology Research Division, Vanderbilt University, Nashville, TN, USA*
[d] *Department of Biophysical Genetics, Kanazawa University Graduate School of Medical Science, Kanazawa, Ishikawa, Japan*

ARTICLE INFO

Article history:
Received 12 January 2010
Received in revised form 2 October 2010
Accepted 5 October 2010
Available online 13 October 2010

Keywords:
Ion channels
Long-QT syndrome
Drugs
Electrophysiology
Hypokalemia

ABSTRACT

The acquired long QT syndrome (aLQTS) is frequently associated with extrinsic and intrinsic risk factors including therapeutic agents that inadvertently inhibit the KCNH2 K^+ channel that underlies the repolarizing I_{Kr} current in the heart. Previous reports demonstrated that K^+ channel regulator 1 (KCR1) diminishes KCNH2 drug sensitivity and may protect susceptible patients from developing aLQTS. Here, we describe a novel variant of *KCR1* (E33D) isolated from a patient with ventricular fibrillation and significant QT prolongation. We recorded the KCNH2 current (I_{KCNH2}) from CHO-K1 cells transfected with *KCNH2* plus wild type (WT) or mutant *KCR1* cDNA, using whole cell patch-clamp techniques and assessed the development of I_{KCNH2} inhibition in response to well-characterized KCNH2 inhibitors. Unlike *KCR1* WT, the E33D variant did not protect KCNH2 from the effects of class I antiarrhythmic drugs such as quinidine or class III antiarrhythmic drugs including dofetilide and sotalol. The remaining current of the KCNH2 WT + KCR1 E33D channel after 100 pulses in the presence of each drug was similar to that of KCNH2 alone. Simulated conditions of hypokalemia (1 mM $[K^+]_o$) produced no significant difference in the fraction of the current that was protected from dofetilide inhibition with KCR1 WT or E33D. The previously described α-glucosyltransferase activity of KCR1 was found to be compromised in KCR1 E33D in a yeast expression system. Our findings suggest that *KCR1* genetic variations that diminish the ability of KCR1 to protect KCNH2 from inhibition by commonly used therapeutic agents constitute a risk factor for the aLQTS.

1. Introduction

The long QT syndrome (LQTS) can be of the acquired form, which is characterized by pathogenic excessive prolongation of the QT interval, with risk for torsade de pointes (TdP) upon exposure to an environmental stressor [1]. A minority (less than 10%) of probands with the drug-induced acquired LQTS (aLQTS) are known to be affected by a subclinical congenital syndrome [1]. Thus, a subset of aLQTS patients carry mutations in *KCNQ1*, *KCNH2*, *KCNE1*, *KCNE2*, and *SCN5A* [2–6]. Among them, KCNH2 plays an important role in cardiac repolarization because KCNH2 channels conduct the rapid delayed rectifier K^+ current (I_{Kr}) which is an important component of phase 3 repolarization of cardiac muscle.

Multiple proteins are known to affect the function of KCNH2 in heterologous systems. MiRP1 encoded by *KCNE2* is thought to regulate KCNH2 in the human heart; MinK encoded by *KCNE1* may also modulate KCNH2 in vivo; 14-3-3ε binding to KCNH2 channels shifts the activation curve towards more hyperpolarized potentials; GM130, a Golgi-associated protein, interacts with KCNH2 as the channel is transported between the endoplasmic reticulum and the plasma membrane [7–10]. These proteins that influence KCNH2 function must also be considered candidates for arrhythmia causing genes. We previously identified a protein that accelerated the activation of rat EAG K^+ channels and called it K^+ channel regulator 1 (KCR1) [11]. We also found that KCR1 did not alter KCNH2 current (I_{KCNH2}) properties in heterologous systems, but that overexpression protected I_{KCNH2} from blockade by dofetilide, sotalol, or quinidine [12]. We subsequently demonstrated that in mammalian cells, the yeast α-glucosyltransferase, *ALG10*, which is the closest homolog of *KCR1*, also inhibited dofetilide blockade of I_{KCNH2} [13]. The I447V variant of *KCR1* occurred in 1.1% of patients with drug-induced TdP, compared with 7% of controls, suggesting that the presence of valine

* Corresponding author. Division of Cardiovascular Medicine, Kanazawa University Graduate School of Medical Science, 13-1, Takara-machi, Kanazawa , Ishikawa 920-8640, Japan. Fax: +81 76 234 4251.
E-mail address: kenshi@med.kanazawa-u.ac.jp (K. Hayashi).

0022-2828/$ – see front matter © 2010 Elsevier Ltd. All rights reserved.
doi:10.1016/j.yjmcc.2010.10.007

in this position may exert a protective effect [14]. In a heterologous expression system, the I447V variant was more effective at protecting KCNH2 against dofetilide inhibition than wild type (WT) KCR1 [14]. Thus, we concluded that KCR1 can modulate the risk of drug-induced cardiac arrhythmias. In the present study, we identified a *KCR1* genetic variant (E33D) in a patient who suffered ventricular fibrillation and QT prolongation, and characterized electrophysiological alterations and changes in drug sensitivity of this variant. We also evaluated the enzymatic α-glycosyltransferase function of this variant in a yeast expression system.

2. Methods

2.1. Study population and mutation analysis

We evaluated 14 patients (8 females and 6 males, mean age 66 ± 24 years) with aLQTS, which was defined as a prolonged corrected QT interval (QTc > 550 ms) and an episode of TdP or ventricular fibrillation induced by drugs or associated with other underlying conditions. To identify gene mutations, we performed genetic analysis after obtaining written informed consent from the patients in accordance with the guidelines of the Bioethical Committee on Medical Research of Kanazawa University. Genomic DNA was purified from white blood cells and amplified using a standard polymerase chain reaction (PCR) method. Single-strand conformational polymorphism (SSCP) analysis of the amplified DNA was performed to screen for mutations in all exons of *KCR1*, *KCNQ1*, *KCNH2*, *SCN5A*, *KCNE1*, and *KCNE2*. Normal and aberrant mutant DNA strands identified in SSCP analysis were isolated and sequenced using an ABI PRISM 310 Genetic Analyzer (PE Applied Biosystems, Foster City, CA).

2.2. Plasmid constructs

The *KCNH2* cDNA was subcloned into the mammalian expression vector pSI (Promega, Madison, WI), as described previously [15]. The human *KCR1* cDNA was subcloned into the pCGI vector for bicistronic expression with enhanced green fluorescent protein (GFP). For expression in yeast, *ALG10* and *KCR1* WT were subcloned into the pGPD426 yeast shuttle vector that allows for selection on uracil-deficient media, as described previously [13,16]. The *KCR1* E33D cDNA was constructed by an overlap extension strategy [17]. The sequence of the *KCR1* E33D cDNA was confirmed by DNA sequence analyses using 7 primer pairs. The cDNA was sequenced in its entirety after transfer into the yeast vector and no other modifications due to mutagenesis were identified.

2.3. Electrophysiology

CHO-K1 cells (RIKEN BRC Cell Bank, Tsukuba, Japan) were cultured in Ham's F-12 medium (HyClone, Logan, UT) supplemented with 10% fetal bovine serum and 1% penicillin-streptomycin in an incubator with a humidified atmosphere of 5% CO_2 at 37°C. CHO-K1 cells were transiently co-transfected with the following combinations of vectors: *KCNH2* WT cDNA (1 μg) plus green fluorescent protein (GFP) in pCGI vector (1 μg), *KCNH2* WT (1μg) plus *KCR1* WT (1μg), *KCNH2* WT (1μg) plus *KCR1* E33D (1 μg), or *KCNH2* WT (1 μg) plus *KCR1* WT (0.5 μg) plus *KCR1* E33D (0.5 μg), using FuGENE 6 Transfection Reagent (Roche, Indianapolis, IN). Cells displaying green fluorescence 48–72 hours after transfection were subjected to electrophysiological analysis.

Membrane currents were studied using the whole cell patch clamp technique with an amplifier, Axopatch-200B (Axon Instruments, Foster City, CA), at room temperature (23–25 °C). Electrode resistances ranged from 3 to 5 MΩ when filled by pipette with an intracellular solution containing: 110 mM KCl, 5 mM K_2ATP, 2 mM $MgCl_2$, 10 mM HEPES, and 5 mM K_4BAPTA at pH 7.2. During recording, the bath solution contained 140 mM NaCl, 5.4 XCl mM (X = sum of K^+ and *N*-methyl-D-glucamine$^+$ [NMDG]), 2 mM $CaCl_2$, 1.0 mM $MgCl_2$, 10 mM HEPES, and 10 mM glucose, adjusted to pH 7.4 with NaOH. Data acquisition and analysis were performed by a Digidata 1321 A/D converter and pCLAMP8.2 software (Axon Instruments, Foster City, CA).

All pulse protocols are described in the figures and figure legends; the holding potential in all cases was −80 mV. Voltage clamp command pulses were generated and patch clamp data were acquired using pCLAMP8 software (version 8.2, Axon Instruments). Data analysis was carried out using Clampfit (version 8.2, Axon Instruments).

Dofetilide was provided by Pfizer Global Research and Development (Sandwich, UK), and quinidine and D,L-sotalol were purchased from Sigma-Aldrich (St. Louis, MO). After I_{KCNH2} was recorded under control conditions, each drug was added to the bath solution at the indicated concentrations, followed by repetitive depolarizing pulses to +20 mV (2 s) from a holding potential of −80 mV (6 s) and hyperpolarizing pulses to −50 mV (2 s).

All values are expressed as mean ± standard error of the mean (SEM). Differences among these values were evaluated using an analysis of variance (ANOVA) and the unpaired Student's *t*-test where appropriate. A P value of <0.05 was considered to be significant.

2.4. Yeast transformation and Western blot analysis

The method for culturing and transformation of yeast was as described previously [13,18,19]. Equal numbers of yeast cells were inoculated into SD/-ura media plus 1 M Sorbitol and grown for 40 hours to a total density of 2.7×0^7 cells before transformation. *KCR1* WT, *KCR1* E33D or *ALG10* cDNAs were inserted into the pGPD426 vector and the vectors containing these cDNAs or pGPD426 empty vector (control), were transfected into the Alg10-deficient *wbp1-2/alg10* yeast strain YG649. As controls, the WT yeast strain SS328 and untransformed YG649 controls were grown in SD/-ura plus uracil and 1 M Sorbitol and processed in parallel. After transformation, the cells were grown on agar plates containing appropriate selection medium; individual colonies were picked from the plates and grown for 40 hours at 30 °C; the SS328 and untransformed YG649 controls were grown for 18 hours until comparable cell densities were reached, measured by $O.D._{600}$. Protein extracts from yeast cells were prepared for Western blot analysis as described previously [13].

3. Results

3.1. Molecular genetic analyses and clinical characteristics of a patient with a variant of KCR1

Genetic analysis revealed a novel variant of *KCR1* at amino acid position 33 (E33D) in a patient with ventricular fibrillation and QT prolongation (Fig. 1A, Table 1). We did not find this variant of *KCR1* in 200 healthy control individuals or any other mutation in this patient in all exons of *KCNQ1*, *KCNH2*, *SCN5A*, *KCNE1*, and *KCNE2*. However, we identified three mutations in *KCNH2* in three other patients: M124T and 527 ins C (R176fsX331) both in the N-terminus, and H492Y in the S2/S3 region (Table 1). In total, 4 out of 14 patients with aLQTS (29%) carried gene mutations. We also identified four polymorphisms: *KCNQ1* G643S, *SCN5A* H558R, *SCN5A* R1193Q, and *KCNE1* D85N (Table 1).

The patient with *KCR1* E33D was a 70-year-old man whose mother had died suddenly of unexplained causes. The patient had been treated with manidipine, kallidinogenase and bezafibrate for hypertension and hyperlipidemia since age 65. He suddenly fell unconscious in a restaurant and was found to have ventricular fibrillation by the emergency crew (Fig. 1B). After prompt defibrillation, he was brought to a hospital by ambulance. Blood chemistry results in the emergency room indicated hypokalemia (3.1 mEq/l). The ECGs which were recorded after admission indicated prolonged QTc (Fig. 1C). Metoprolol 60 mg and mexiletine 300 mg were initiated on the

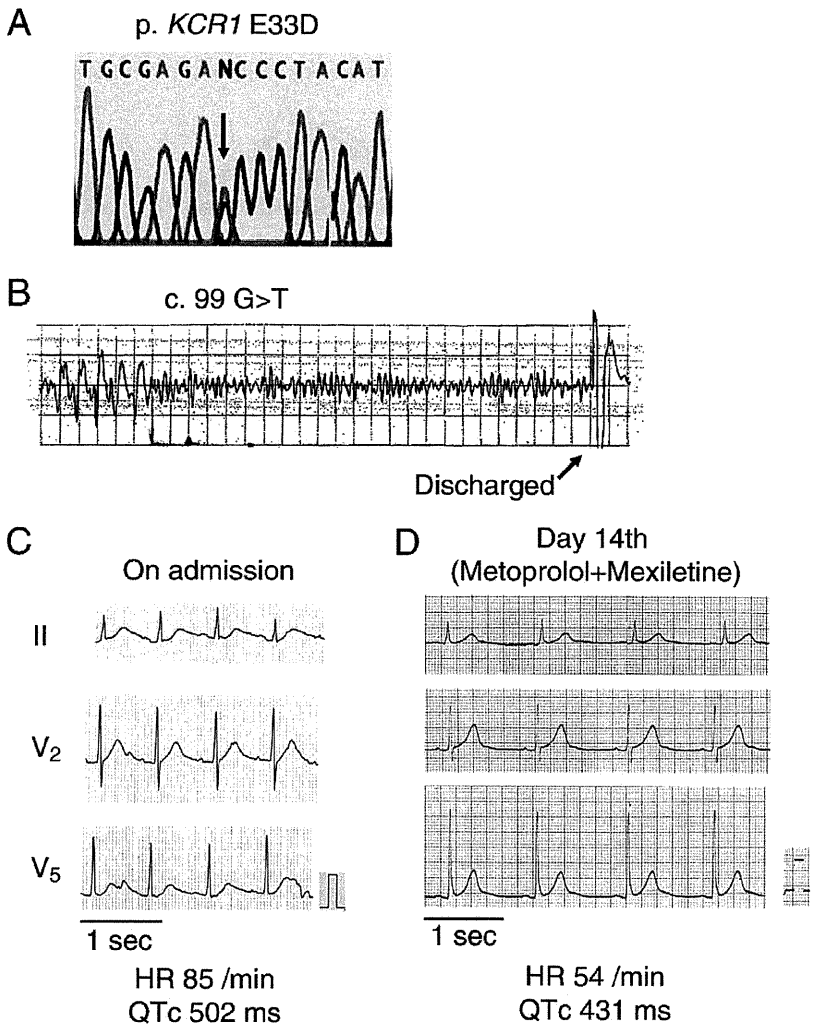

Fig. 1. Genetic analysis and electrocardiograms. (A) DNA sequence of *KCR1* showing the base sequence around the coding region of amino acid residue 33 in the patient with ventricular fibrillation and significant QT prolongation. (B) Electrocardiographic tracing during cardiopulmonary arrest. ECG shows ventricular fibrillation and discharge waveform by defibrillator. (C) and (D) ECGs recorded during hospital stay. ECG on admission shows prolonged QTc interval of 502 ms (C). In contrast, ECGs at day 14 after initiation of metoprolol and mexiletine show a normalized QTc interval (D).

Table 1
Mutations and polymorphisms identified in this study.

Gene	Nucleotide Change	Amino acid Change
Mutations		
KCR1	G99T	E33D
KCNH2	T371C	M124T
KCNH2	527 ins C	R176fsX331
KCNH2	C1474T	H492Y
Polymorphisms		
KCNQ1	G1927A	G643S
SCN5A	A1673G	H558R
SCN5A	G3578A	R1193Q
KCNE1	G253A	D85N

second hospital day, and an ECG on his 14th day of hospitalization showed that the QT interval had normalized (QTc 431 ms) (Fig. 1D).

3.2. Electrophysiological findings of KCNH2 channels co-expressed with KCR1 E33D

We previously reported that KCR1 had no effect on the activation gating or voltage dependence of inactivation [12]. Here, we evaluated the effect of the KCR1 E33D variant on KCNH2 channel activity. Fig. 2A shows representative current traces recorded in CHO cells expressing KCNH2 WT alone, KCNH2 WT + KCR1 WT, or KCNH2 WT + KCR1 E33D. Fig. 2B shows the current–voltage relationship for the peak activating currents, which was similar in all three conditions. The amplitude of the tail currents was plotted as a function of the test potential and the curve was fitted to a Boltzmann function. The voltage at which the tail current was half activated ($V_{1/2}$) was 4.35 ± 1.8 mV for KCNH2 WT alone ($n = 14$), 1.0 ± 1.8 mV for KCNH2 WT + KCR1 WT ($n = 16$), and 4.0 ± 1.6 mV for KCNH2 WT + KCR1 E33D ($n = 16$, P = NS compared with KCNH2 WT

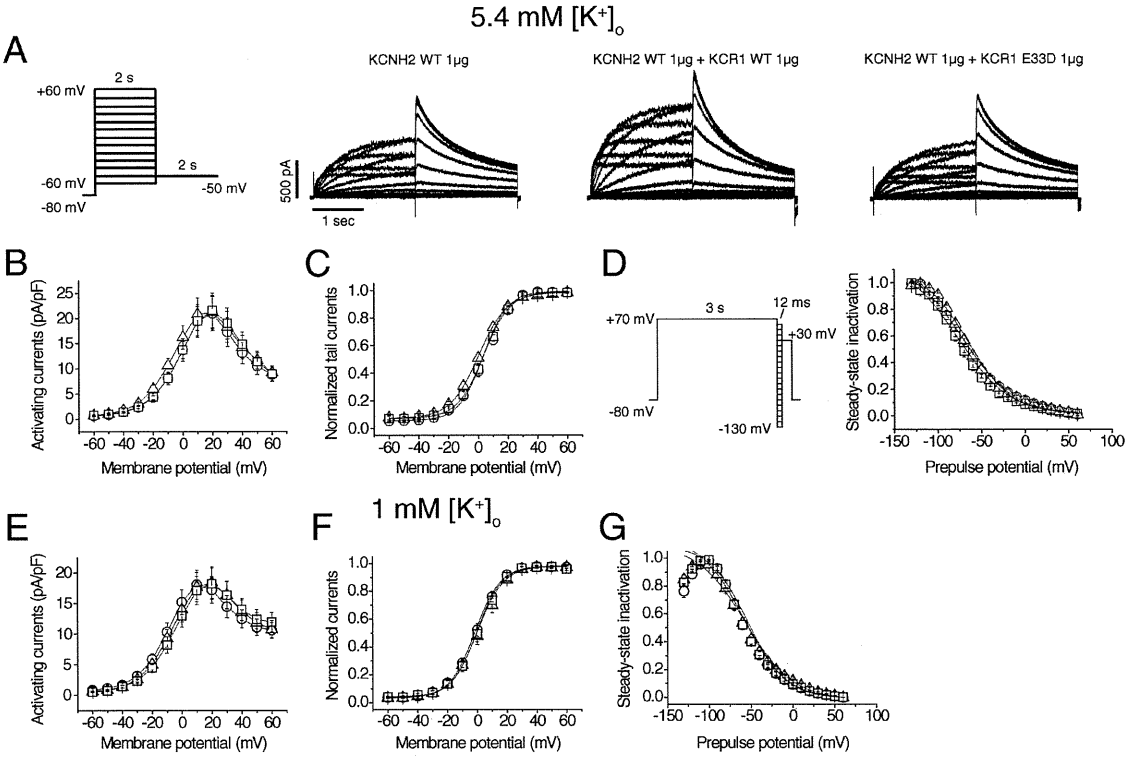

Fig. 2. Functional characterization of KCNH2 channels co-expressed with KCR1 E33D at varying $[K^+]_o$. (A) The activation voltage-clamp protocol (left). Representative currents expressed in CHO-K1 cells at 5.4 mM $[K^+]_o$, transfected with 1 μg *KCNH2* WT alone, 1 μg *KCNH2* WT plus *KCR1* WT, and 1 μg *KCNH2* WT plus 1 μg *KCR1* E33D variant. (B) *I–V* relationships for the peak currents in CHO-K1 cells at 5.4 mM $[K^+]_o$. *N* ranged from 14 to 16. (C) Normalized *I–V* relationships for mean amplitudes of tail currents at 5.4 mM $[K^+]_o$ in 14–16 experiments. (D) Voltage dependence of inactivation determined by a three-step protocol (left). Current amplitude at test potential was normalized and plotted against prepulse potentials. Normalized steady-state inactivation curves of expressed currents in CHO-K1 cells at 5.4 mM $[K^+]_o$ in 4–5 experiments. (E) *I–V* relationships for the peak currents in CHO-K1 cells at 1.0 mM $[K^+]_o$. *N* ranged from 15 to 17. (F) Normalized *I–V* relationships for mean amplitudes of tail currents at 1.0 mM $[K^+]_o$ in 13–16 experiments. (G) Normalized steady-state inactivation curves of expressed currents in CHO-K1 cells at 1.0 mM $[K^+]_o$ in 9–10 experiments. ○, *KCNH2* WT 1 μg; △, *KCNH2* WT 1 μg + *KCR1* WT 1 μg; □, *KCNH2* WT 1 μg + *KCR1* E33D 1 μg.

alone), indicating that KCR1 E33D did not affect the voltage dependence of activation of the KCNH2 WT channel (Fig. 2C). The voltage-dependent distribution of channels between the open and inactivated states was also examined using a 3-pulse clamp protocol (Fig. 2D). The peak tail current amplitude was measured in the final step to +30 mV and was plotted as a function of the preceding test potential. The $V_{1/2}$ for the voltage dependence of steady-state channel availability was −74.5 ± 7.8 mV ($n=5$) for KCNH2 WT alone, −70.0 ± 2.6 mV ($n=5$) for KCNH2 WT + KCR1 WT, and, −75.2 ± 4.1 mV ($n=4$) for KCNH2 WT + KCR1 E33D, indicating that the E33D variant did not affect the voltage dependence of steady-state inactivation.

Hypokalemia is a recognized risk factor for the LQTS, and because the index patient was slightly hypokalemic at the time of emergency room admission, it was important to ascertain the influence of extracellular K^+ concentration ($[K^+]_o$) in this paradigm [20]. We therefore repeated the same experiments in low $[K^+]_o$(1 mM). The results are shown in Fig. 2E–G. Fig. 2E shows the current–voltage relationships for activating peak currents during depolarizing pulses in 1 mM $[K^+]_o$. The voltage at which the tail current was half activated ($V_{1/2}$) was -0.52 ± 1.8 mV for KCNH2 WT alone (n = 16), 1.3 ± 2.4 mV for KCNH2 WT + KCR1 WT ($n=15$), and 1.1 ± 2.1 mV for KCNH2 WT + KCR1 E33D ($n=13$, P = NS compared with KCNH2 WT alone), (Fig. 2F). The $V_{1/2}$ for the voltage dependence of steady-state channel availability (Fig. 2G) was −54.8 ± 3.4 mV ($n=9$) for KCNH2 WT, −55.7 ± 3.8 mV ($n=10$) for KCNH2 WT + KCR1 WT, and, −55.2 ± 2.4 mV ($n=10$) for KCNH2 WT + KCR1 E33D. The fast and slow deactivation time constants of tail currents in 1 mM $[K^+]_o$ measured after a 2 sec depolarizing step to +20 mV and repolarization to potentials between −40 and −80 mV were comparable in cells transfected with KCNH2 WT alone ($n=15$), KCNH2 WT + KCR1 ($n=13$), and WT KCNH2 WT + KCR1 E33D ($n=12$) (data not shown). These results show that varying $[K^+]_o$ does not significantly alter the response of basal KCNH2 current to KCR1 WT or E33D.

3.3. Unlike KCR1 WT, E33D does not modulate sensitivity of I_{KCNH2} to channel blockers

We next evaluated whether the KCR1 E33D variant modulated drug sensitivity of the I_{KCNH2} current (Fig. 3). Representative traces of the KCNH2 WT tail currents recorded at −50 mV are shown in Fig. 3A. As reported previously, co-expression of KCR1 WT with KCNH2 WT protected I_{KCNH2} from the onset of inhibition by dofetilide. In contrast, co-expressing the E33D variant with KCNH2 WT had no significant effects on response to dofetilide (Fig. 3A and B). Following 100 pulses applied every 10 sec after application of 50 nM dofetilide in 5.4 mM $[K^+]_o$, 72 ± 4% ($n=13$) of the KCNH2 WT + KCR1 WT current remained, whereas only 51 ± 4% ($n=14$) of the KCNH2 WT + KCR1 E33D current remained ($P<0.05$ vs. KCNH2 WT + KCR1 WT) (Fig. 3B and D). The amount of inhibition of the KCNH2 WT + KCR1 E33D current was comparable to that of KCNH2 WT alone (53 ± 4%, $n=11$) (Fig. 3B and D). We estimated the IC_{50} for dofetilide to be 67 nM in the presence of the KCR1 E33D variant vs.

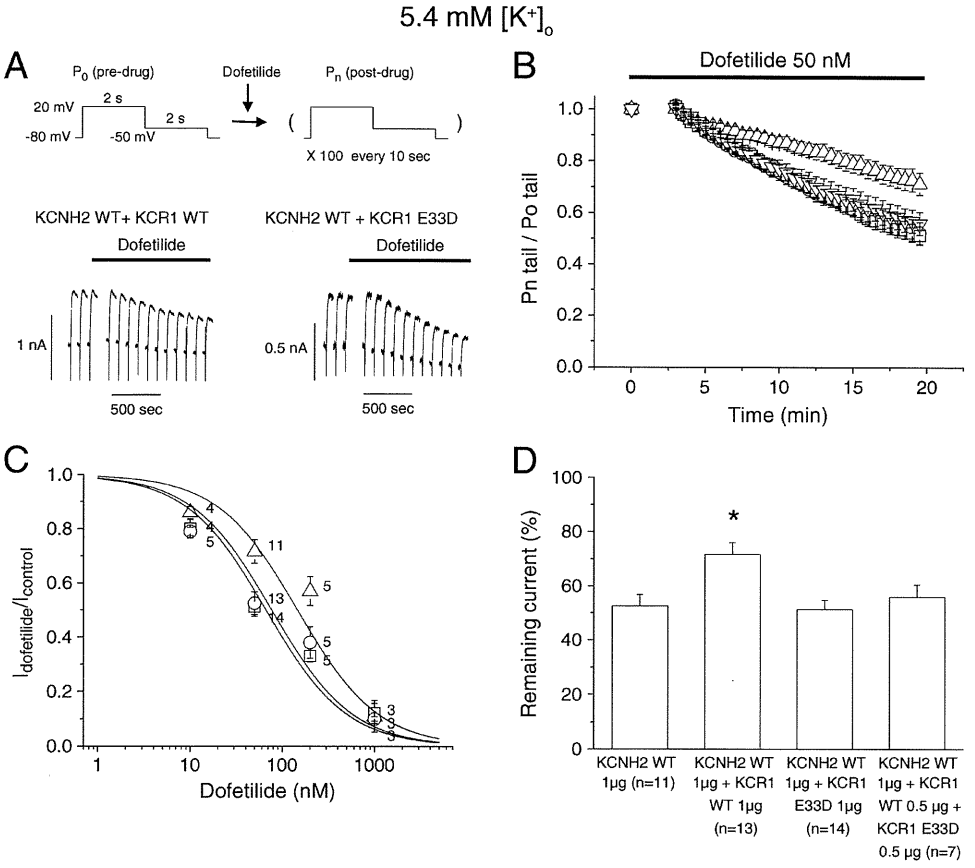

Fig. 3. Effects of KCR1 WT and E33D on dofetilide inhibition of KCNH2 current in CHO-K1 cells at 5.4 mM $[K^+]_o$. (A) Representative currents for KCNH2 WT plus KCR1 WT (bottom, left), and KCNH2 WT plus KCR1 E33D (bottom, right) during repetitive depolarizing pulses (top) in the presence of dofetilide. (B) Relative peak tail currents during repetitive pulses in the presence of dofetilide. *N* ranged from7 to 14. (C) Concentration dependence of blockade. Mean data were fitted to a logistic expression $(1/1+\{[D]/IC50\}^n)$, where [D] is dofetilide concentration and *n* is the Hill coefficient. (D) Percentage of outward current remaining after 100 pulses applied every 10 sec of 50 nM dofetilide perfusion. *$P<0.05$ versus KCNH2 WT, KCNH2 WT + KCR1 E33D, and KCNH2 WT + KCR1 E33D + KCR1 WT. ○, *KCNH2* WT 1 μg; △, *KCNH2* WT 1 μg + *KCR1* WT 1 μg; □, *KCNH2* WT 1 μg + *KCR1* E33D 1 μg; ▽, *KCNH2* WT 1 μg + *KCR1* WT 0.5 μg + *KCR1* E33D 0.5 μg.

146 nM in the presence of KCR1 WT (Fig. 3C). The IC_{50} of E33D was similar to that of KCNH2 WT alone (76 nM).

Because the patient with KCR1 E33D was heterozygotic for the mutation, we evaluated the effects of co-expressing WT and KCR1 variant on dofetilide sensitivity. Unlike KCR1 WT alone, co-expressing KCNH2 with KCR1 WT and E33D enhanced the drug blockade of I_{KCNH2} (Fig. 3B). Fig. 3D shows current remaining after 100 pulses applied every 10 sec after application of 50 nM dofetilide. The remaining current of KCNH2 WT + KCR1 WT + KCR1 E33D was 56 ± 5% ($n=7$), which was similar to that of KCNH2 WT alone, and significantly smaller than that of KCNH2 WT + KCR1 WT ($P<0.05$).

Fig. 4A plots the development of dofetilide blockade in 1 mM $[K^+]_o$ during a train of depolarizing pulses. Similar to the development of dofetilide blockade in 5.4 mM $[K^+]_o$ (Fig. 3), co-expressing KCNH2 WT and KCR1 WT slowed drug blockade of I_{KCNH2} compared to expressing KCNH2 WT alone or co-expressing KCNH2 WT and KCR1 E33D (Fig. 4A). The effect of co-expression of KCR1 WT and E33D on dofetilide blockade of I_{KCNH2} was intermediate between KCR1 WT alone and E33D alone (Fig. 4A). Fig. 4B shows the current remaining after 100 pulses after application of 50 nM dofetilide in 1 mM $[K^+]_o$. The remaining current of the KCNH2 WT + KCR1 E33D channel was 39 ± 5% ($n=8$), which was similar to that of the KCNH2 WT channel (37 ± 6%, $n=7$), and was significantly smaller than that of the KCNH2 WT + KCR1 WT channel (57 ± 4%, $n=7$, $P<0.05$). The amount of inhibition of the KCNH2 WT + KCR1 WT + KCR1 E33D current was 47 ± 3% ($n=7$), which was not significantly smaller than that of the KCNH2 WT + KCR1 WT current ($P<0.1$). In addition, the remaining current of the KCNH2 WT + KCR1 E33D channel after application of 50 nM dofetilide in 1 mM $[K^+]_o$ was significantly smaller than that in 5.4 mM $[K^+]_o$ (39 ± 5% versus 56 ± 5%, $P<0.05$). Thus, in low $[K^+]_o$, the same general effects of KCR1 WT and KCR1 E33D were observed, although overall levels of current remaining were smaller in 1 mM than in 5.4 mM $[K^+]_o$.

To determine if the effect of the KCR1 E33D variant can be generalized, we studied the effect of KCR1 on I_{KCNH2} blockade by quinidine and D,L-sotalol. Fig. 5A plots the development of quinidine blockade in the standard bath solution during repetitive depolarizing pulses. Quinidine at 2 μM produced rapid blockade, reaching equilibrium level of I_{KCNH2} inhibition within the first few test pulses. Contrary to KCR1 WT, KCR1 E33D did not reduce the extent of quinidine blockade (Fig. 5A and B); by the second pulse, the remaining current of the KCNH2 WT + KCR1 E33D channel was 56 ± 3% ($n=8$), which was similar to that of the KCNH2 WT channel (52 ± 3%, $n=7$) and that of the KCNH2 WT + KCR1 WT + KCR1 E33D channel (58 ± 4%, $n=10$), and was significantly smaller than that of the KCNH2 WT + KCR1 WT channel (73 ± 4%, $n=8$, $P<0.05$ vs. the

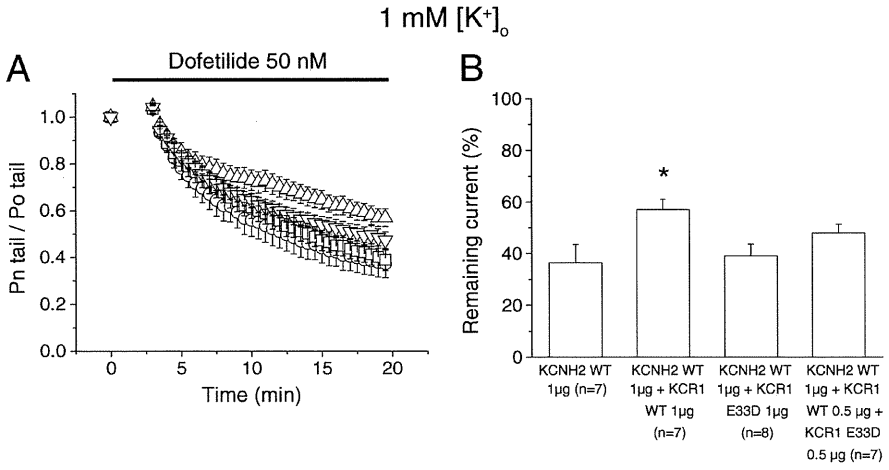

Fig. 4. Time-dependent blockade of KCNH2 current by dofetilide in low $[K^+]_o$. (A) Relative peak tail currents during repetitive pulses in the presence of 50 nM dofetilide for KCNH2 WT alone (○, $n=6$), KCNH2 WT plus KCR1 WT (△, $n=7$), KCNH2 WT plus KCR1 E33D (□, $n=8$), and KCNH2 WT plus KCR1 WT plus KCR1 E33D (▽, $n=7$). $[K^+]_o$ was 1.0 mM in these experiments. (B) Percentage of outward current remaining after 100 pulses applied every 10 sec of 50 nM dofetilide perfusion. *$P<0.05$ versus KCNH2 WT and KCNH2 WT plus KCR1 E33D.

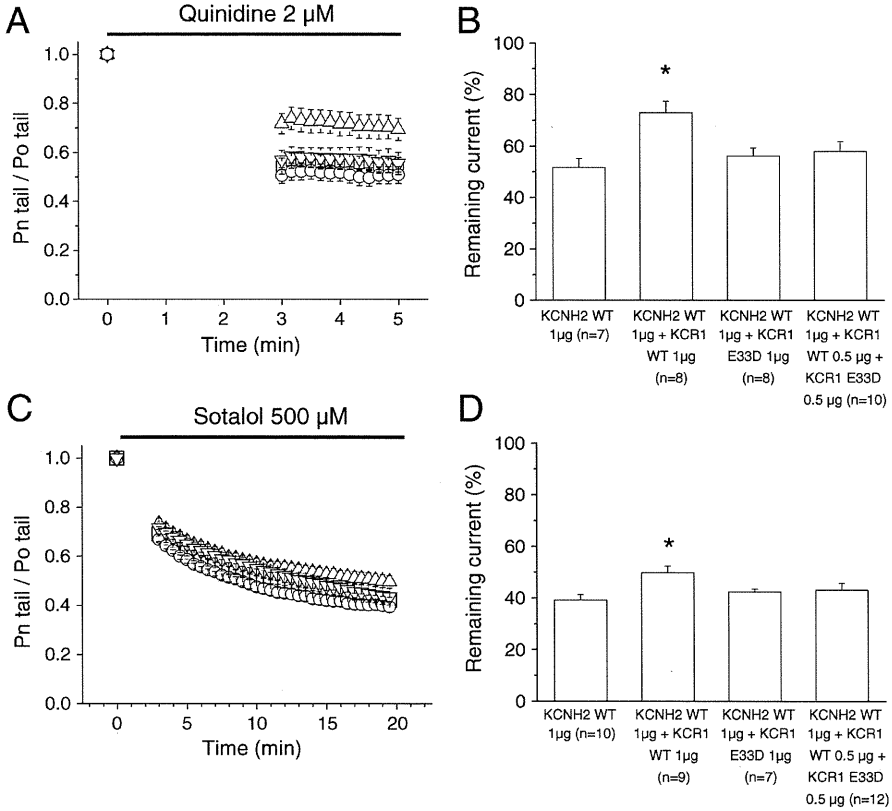

Fig. 5. Time-dependent blockade of KCNH2 current by quinidine and D,L-sotalol in the standard bath solution (5.4 mM $[K^+]_o$) (A) Relative peak tail currents during repetitive pulses in the presence of 2 μM quinidine. N ranged from 7 to 10. (B) Percentage of outward current remaining after 100 pulses applied every 10 sec of 2 μM quinidine perfusion. *$P<0.05$ versus KCNH2 WT and KCNH2 WT plus KCR1 E33D. (C) Relative peak tail currents during repetitive pulses in the presence of 500 μM D,L-sotalol. *N* ranged from 7 to 12. (D) Percentage of outward current remaining after 100 pulses applied every 10 sec of 500 μM sotalol perfusion. *$P<0.05$ versus KCNH2 WT and KCNH2 WT plus KCR1 E33D. ○, *KCNH2* WT 1 μg; △, *KCNH2* WT 1 μg + *KCR1* WT 1 μg; □, *KCNH2* WT 1 μg + *KCR1* E33D 1 μg; ▽, *KCNH2* WT 1 μg + *KCR1* WT 0.5 μg + *KCR1* E33D 0.5 μg.

KCNH2 WT + KCR1 E33D channel). Fig. 5C shows the development of sotalol blockade in the standard bath solution. D,L-sotalol blockade developed rapidly and reached an equilibrium level of I_{KCNH2} inhibition over minutes. I_{KCNH2} remaining after 100 pulses of 500 μM D,L-sotalol exposure was 42 ± 1% of the predrug control for the KCNH2 WT + KCR1 E33D channel ($n=7$), which was comparable to 39 ± 2% for the KCNH2 WT channel ($n=10$), but 50 ± 3% for the KCNH2 WT + KCR1 WT channel ($n=9$) ($P<0.05$ vs. the KCNH2 WT + KCR1 E33D channel or vs. the KCNH2 WT channel) (Fig. 5C and D). The amount of inhibition of the KCNH2 WT + KCR1 WT + KCR1 E33D current was 43 ± 2% ($n=12$), which was not significantly smaller than that of the KCNH2 WT + KCR1 WT current ($P<0.1$).

3.4. Unlike WT, the E33D variant does not rescue a growth defect caused by alg10 deficiency in yeast and does not possess α-glucosyltransferase activity

The closest known homolog of *KCR1* is the yeast α-glucosyltransferase, *ALG10*. We previously demonstrated that the mammalian *KCR1* cDNA, when introduced into yeast, is able to rescue a growth defect in the alg10-deficient yeast strain YG649 [13]. Fig. 6 reiterates that this growth defect is complemented by transformation with a yeast vector expressing *ALG10* (Fig. 6A, Section 3) or *KCR1* WT (Fig. 6A, Section 4). In contrast, cells transformed with vector alone (Section 2) or with the E33D variant (Section 5) exhibited little or no growth in the same time period, indicating that the E33D variant has lost the ability to rescue the growth defect of the YG649 strain.

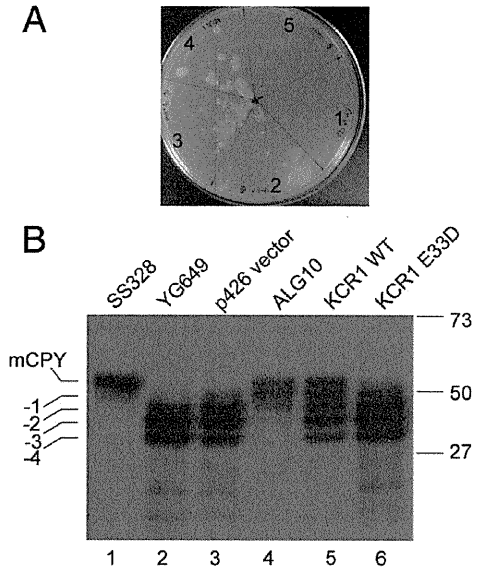

Fig. 6. Unlike KCR1 WT, KCR1 E33D fails to rescue the *alg10* defect in yeast. (A) The alg10-deficient yeast strain YG649 (*wbp1-2/alg10*) was either untransformed (1), or transformed with the E33D variant (5), empty vector (2), vector plus *KCR1* WT (4), vector plus *ALG10* (3), and plated on SD/-ura selective growth media. The vector carries a URA selection marker to facilitate identification of transformants. (B) Whole cell protein extracts were prepared from the transformed and control yeast strains and processed for Western blot analysis by electrophoresis on 10% SDS polyacrylamide gels. The gels were subjected to Western blot analysis using an anti-CPY antibody. Lane 1, SS328 (WT), the mature, fully glycosylated form of CPY (mCPY) is produced preferentially; lane 2, the YG649 *wbp1-2/alg10* mutant yeast strain mainly produces the incompletely glycosylated −4, −3, and −2 forms of CPY; lane 3, YG649 transformed with empty vector; lane 4, transformed with *ALG10*; lane 5, transformed with *KCR1* WT; lane 6, transformed with E33D variant of *KCR1*. Molecular mass markers are indicated on the right. The positions of the −4, −3, −2, −1 and mature glycosylated forms of CPY are indicated on the left. Three independent experiments produced comparable results.

The α-glucosyltransferase activity of ALG10 and KCR1 can be conveniently measured by Western blot analysis of the ALG10 substrate carboxypeptidase Y (CPY), which is endogenous to yeast [13]. Since CPY contains four N-linked oligosaccharides, it migrates at five different positions on an SDS polyacrylamide gel [19]. We found that ALG10 and KCR1 are functional homologs in YG649, confirming our previous results [13]. They both produced the −1 and fully glycosylated forms of CPY (mCPY) (Fig. 6B, lanes 4 and 5, respectively), as well as the incompletely glycosylated forms that are preferentially produced by the alg10-deficient YG649 mutant (Fig. 6B, lanes 2 and 3). In contrast, the E33D variant (Fig. 6B, lane 6) did not produce the fully glycosylated form (mCPY), thus functioning at a level similar to YG649 transformed with vector alone (Fig. 6B, lane 3). This indicates that the E33D mutation results in a loss of KCR1-associated α- glucosyltransferase activity in yeast.

4. Discussion

The aLQTS has many possible underlying causes, the most common of which are side effects from medications administered for unrelated conditions. Underlying structural heart disease is also a risk factor for the aLQTS [1]. Several reports have described the role of genetic variants in aLQTS [5–7,21,22]. Unrecognized congenital LQTS and its predisposing DNA polymorphisms were identified as risk factors for drug-induced TdP [1]. These genetic variants decreased or altered heterologously expressed currents or increased the drug sensitivity of I_{KCNH2} [5,7,21].

We have previously reported that KCR1 is expressed in human heart, modulates drug blockade of I_{KCNH2} through the cellular glycosylation pathway, and functions as an α-1,2 glucosyltransferase [12,13]. In control populations, basal levels of KCR1 expression in the heart provide a level of protection against inhibition of I_{Kr} by therapeutic agents. Indeed, polymorphisms in *KCR1* (I447V) exist that appear to improve the ability of KCR1 to prevent drug-induced LQTS [14]. In contrast, in this study, we showed that the KCR1 E33D did not protect KCNH2 from the effects of well-characterized KCNH2 inhibitors, including the class I antiarrhythmic quinidine, and the class III antiarrhythmics, dofetilide and sotalol (Figs. 3–5). The KCR1 E33D variant may enhance susceptibility to aLQTS by decreasing the biochemical activity of KCR1 (α-glucosyltransferase activity, see Fig. 6) and therefore lowering the ability of KCR1 to protect I_{Kr} from the effects of the drug. Because the patient with KCR1 E33D is heterozygotic for the variant, we evaluated the effect of co-expression of KCR1 WT and E33D on the dofetilide blockade of I_{KCNH2}. Co-expressing KCNH2 with KCR1 E33D and KCR1 WT to approximate the heterozygous condition enhanced the effects of dofetilide on the KCNH2 current, similar to expressing KCNH2 alone or co-expressing KCNH2 and KCR1 E33D (Figs. 3B, D, 4, and 5).

In a prior study using computational modeling, we showed that KCNH2 blockade, sufficient to evoke action potential prolongation and development of early after-depolarizations could be reversed by KCR1 effects on I_{KCNH2} [13]. The present study shows that the effects of dofetilide on the I_{KCNH2} current were not reduced by co-expression of KCR1 E33D alone or KCR1 WT and E33D. This suggests that KCR1 E33D may be proarrhythmic when normal KCNH2 function is diminished.

We further evaluated the effect of the variant versus WT KCR1 on KCNH2 currents at different potassium concentrations because the patient with KCR1 E33D was found to be hypokalemic at admission to a hospital. The remaining current of the KCNH2 WT + KCR1 E33D channel after application of 50 nM dofetilide in 1 mM $[K^+]_o$ was significantly smaller than that in 5.4 mM $[K^+]_o$ (Figs. 3 and 4). Lowering the extracellular potassium concentration decreases the magnitude of I_{Kr} and of outward KCNH2 K^+ currents [23,24]. Further, raising serum $[K^+]_o$ to the high normal range can normalize QT prolongation in some congenital long QT patients with KCNH2